

How useful are progressive vector diagrams for studying coastal ocean transport?

Daniel F. Carlson¹, Philip A. Muscarella², Hezi Gildor^{1*}, Bruce L. Lipphardt, Jr.², and Erick Fredj³

¹Department of Environmental Science, Weizmann Institute of Science, Rehovot, Israel

²College of Earth, Ocean, and Environment, University of Delaware, Newark, DE, USA

³Department of Computer Science, Jerusalem College of Technology, Jerusalem, Israel

Abstract

Progressive vector diagrams (PVDs) have been used to estimate transport in the coastal ocean from point measurements of velocity time series, although they strictly only approximate true particle trajectories in regions where the currents are spatially uniform. Currents in most coastal regions vary significantly in both space and time, making coastal transport estimates from PVDs questionable. Here, we used synoptic surface currents measured over periods of several months by HF radars in two coastal areas with distinctly different circulation features (the Gulf of Eilat, a deep, semi-enclosed basin, and the Delaware Bay mouth, a coastal estuarine outflow) to assess the time scales over which PVD paths computed from velocity time series at fixed points separate from particle trajectories computed from two-dimensional measured horizontal currents that vary in both space and time. In both study regions, PVDs and particle trajectories separate by 1 km over a mean time period of 7–10 h with no significant month-to-month variation in either region. The separation time statistics presented here should serve as a strong caution for investigators motivated to estimate transport using only point measurements.

Ocean velocity time series typically consist of orthogonal velocity components (north/east or along/across shore) measured at a fixed location, often using a current meter or current profiler. Typically, current meters measure velocity at a fixed depth, and current profilers measure velocities throughout the water column at high temporal resolution but over a single location. However, costs associated with maintenance and deployment usually limit the number of instruments available to only a few in a given domain and, therefore, the horizontal resolution of a data set is usually very coarse. Whereas velocity time series from a single location can provide important information about the flow at that location,

estimates of the transport of passive particles by the measured flow are often desired. To this end, the flow is taken to be spatially uniform with the observed temporal variability imposed over the entire spatial domain. Under this assumption, a particle path, termed “progressive vector diagram” (PVD), can be constructed by integrating the measured velocities over a specified time interval to obtain a position vector (see Emery and Thomson 2001, p. 165 and 186; Tomczak 2000).

However, uniform spatial currents rarely persist over broad ocean regions, particularly near the coast, so the main assumption on which the PVD analysis rests is most often invalid. The usefulness of PVDs for studying coastal transport problems, then, is questionable. Despite this known limitation, PVDs have been used to examine a number of different coastal physical and biological processes including larvae dispersal (Epifanio et al. 1989; Ben-Tzvi et al. 2007; Fiechter et al. 2008), sediment transport (Ogston et al. 2004), and current variability (Berman et al. 2000). Even in these applications, the limitations of PVDs often emerge. Epifanio et al. (1989), for example, note that PVDs at the Delaware Bay mouth (where tidally dominated currents vary substantially in space) are not good surrogates for particle trajectories. Their figures 2 and 3 show two dramatic examples of PVD paths crossing onto land at the central New Jersey coast during one 46-day period in 1983.

*Corresponding author: E-mail: hezi.gildor@weizmann.ac.il

Acknowledgments

This research was partly funded by the Israel Science Foundation and by NATO SFP982220. D. F. Carlson was supported by a Fulbright grant received in 2007 from the United States–Israel Education Foundation. P. A. Muscarella and B. L. Lipphardt acknowledge support from the Delaware Sea Grant and NOAA support through the US Mid-Atlantic Regional Coastal Ocean Observing System. P. A. Muscarella and B. L. Lipphardt also acknowledge use of the freely available Matlab *OpenMA* toolbox developed by the Central California Coastal Ocean Currents Monitoring Program (COCMP) and the freely available Matlab *m_map* toolbox provided by Rich Pawlowicz at the University of British Columbia.

If transport studies involving PVDs should be restricted only to regions of spatially uniform flow, why have they been used for coastal ocean studies, where the currents are known to vary spatially due to the combined effects of winds, tides, bottom topography, and coastline geometry? The answer is a historical lack of synoptic current measurements. Most historical coastal circulation studies rely on point measurements of velocity time series from current meters or acoustic Doppler current profilers. Point measurements provide an incomplete picture of the spatially varying flow features inherent in coastal regions, making it natural to question their ability to describe transport in the vicinity of the sensors. Because little is typically known about the spatial scales of velocity variability in the neighborhood of in situ sensors, the time and space scales over which PVDs might provide useful transport estimates from sensor measurements could not be determined previously.

Over the past few decades, high-frequency (HF) radar has emerged as a useful tool for measuring synoptic near-surface currents near the coast at high spatial and temporal resolutions (Barrick et al. 1985; Gurgel et al. 1999). Particle trajectories computed from HF radar-measured velocities have been compared with real drifters (Kaplan et al. 2005) and have been used to study submesoscale barriers to mixing (Gildor et al. 2009), pollution releases off the Florida coast (Lekien et al. 2005), synoptic Lagrangian properties (Lipphardt et al. 2006), and Lagrangian coherent structures (Shadden et al. 2009) in Monterey Bay, California. For the first time, coastal oceanographers can use these measurements to directly assess the spatial variability of surface currents and estimate surface transport using particle trajectories integrated directly from the measured velocities. HF radar measurements, then, offer an opportunity to independently assess the appropriate time and space scales over which PVDs might be applied in the coastal ocean. Obviously, if HF radar measurements are available, particle trajectories should be computed directly, and PVDs would not be required. The purpose of a PVD assessment based on HF radar measurements is to gauge the uncertainties associated with their use in coastal areas where HF radar measurements are not available and offer some guidance to investigators who may want to use time series of velocities at a single point to estimate transport. By comparing PVD paths and particle trajectories over several months from two regions with distinctly different circulation characteristics, we explored the range of separation time scales for coastal flows.

Procedures

We used HF radar-measured velocities from two coastal areas to determine the time scales over which PVD paths and particle trajectories begin to separate. Objective mappings of HF radar current measurements in the Gulf of Eilat/Aqaba (September 2005 through September 2006) and at the mouth of the Delaware Bay (January through October 2007) were used to compute both particle trajectories and PVDs to assess separation times. The circulation in the Gulf of Eilat, a deep,

semi-enclosed gulf in the northeast Red Sea, is driven by winds, tides, and thermohaline forcing. On the US east coast, the mouth of the Delaware Bay is a shallow estuarine outflow region dominated by semidiurnal tides with lesser influences due to winds, freshwater outflow, and shelf circulation.

The Gulf of Eilat—The northern terminus of the Gulf of Eilat is a nearly rectangular, deep (~700 m), semi-enclosed basin in the northeast region of the Red Sea measuring roughly 6 km by 10 km (see Fig. 1). This region is bounded by desert mountains that steer the persistent northerly winds along its main axis (Berman et al. 2003). The gulf circulation is driven by tides (predominantly M_2), winds, and thermohaline forcing. Above the thermocline, the circulation is also forced by the flux of water through the Straits of Tiran (Genin and Paldor 1998; Monismith and Genin 2004; Manasrah et al. 2006). In winter, when the seasonal thermocline depth exceeds 600 m, this flux is significantly reduced (Berman et al. 2003; Monismith and Genin 2004). Over a 13-month period (September 2005 through September 2006), two 42-MHz CODAR SeaSondes (see Fig. 1) measured surface currents in the gulf every 30 min with an approximate spatial resolution of 300 m.

The Delaware Bay mouth—The Delaware Bay is an estuary on the US east coast with an 18-km-wide mouth between Cape Henlopen, Delaware, and Cape May, New Jersey (Fig. 2). The bathymetry just outside the bay mouth is quite rugged, including a deep channel across the mouth at the southern side (near Cape Henlopen) and extensive shoals along the mouth's northern side (near Cape May). Annual freshwater outflow typically peaks during the spring runoff in March–May each year. Surface circulation outside the bay mouth varies greatly, driven by the dominant M_2 tide, winds, freshwater outflow, and circulation features on the adjacent continental shelf. Energetic semidiurnal tidal current fluctuations aligned across the bay mouth are always apparent, with amplitudes as large as 80 cm s^{-1} . No other surface flow features persist. From January through October 2007, two 25-MHz CODAR SeaSondes (see Fig. 2) measured surface currents hourly outside the bay mouth with an approximate spatial resolution of 1.5 km.

Objective mapping—Technological and environmental factors often conspire to make HF radar measurements gappy in both space and time. These gaps must be filled before particles can be reliably tracked through any analysis region. Here, spatial gaps at each HF radar measurement time were filled using open-boundary modal analysis (OMA), described by Lekien et al. (2004) for mapping total velocities and by Kaplan and Lekien (2007) for mapping radial velocities. The OMA procedure objectively maps the HF radar measurements using three sets of basis functions that are truncated at a specified spatial resolution. Dirichlet modes (with zero horizontal divergence) represent the flow's vorticity structure. Neumann modes (with zero relative vorticity) account for horizontal divergence. Boundary modes are used to represent the normal flow through the analysis domain open boundaries.

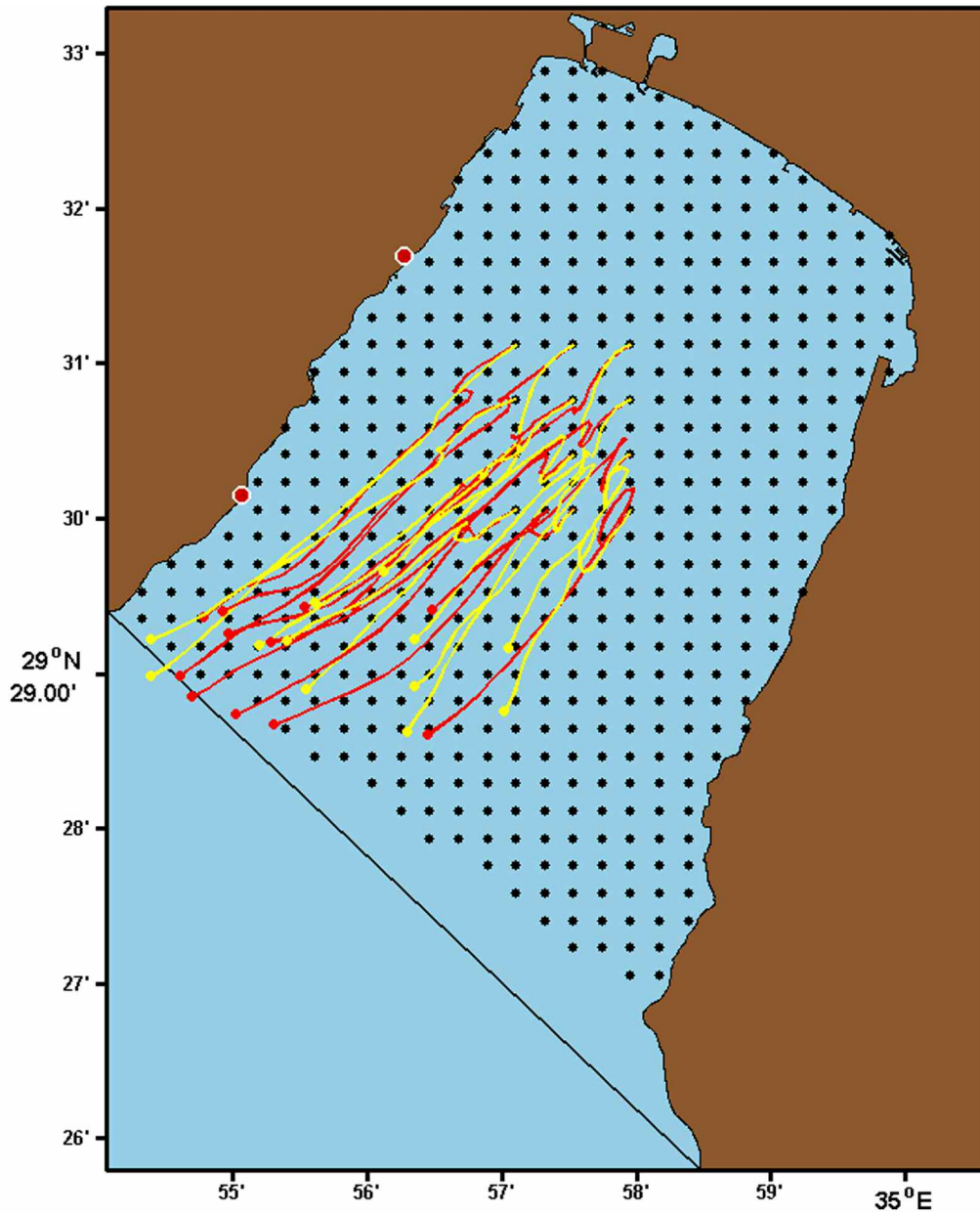


Fig. 1. The Gulf of Eilat and the 510 initial positions (black dots) used to compute trajectories and PVDs for this study. The locations of the two radar sites (red circles) and 12 example trajectories (red lines) and PVDs (yellow lines) are also shown. The PVDs and trajectories were launched at 00:00:00 UT 1 October 2005 and integrated for 12 h.

In the Gulf of Eilat, all measurements exceeding 60 cm s^{-1} were discarded since wave effects occasionally produce unrealistically high velocities near shore. Over the 13-month analysis period, HF radar coverage was typically good, with only modest spatial gaps (mainly along the northern end of the Gulf). Radial velocities were objectively mapped using the procedure of Lekien et al. (2004) as detailed in Lekien and Gildor (2009), with a spatial scale of approximately 350 m. This spatial resolution threshold resulted in a set of 100 Dirichlet modes, 130 Neumann modes, and 40 boundary modes (Lekien and Gildor 2009).

At the Delaware Bay mouth, HF radar spatial coverage over the 10-month analysis period was not as consistent as the Gulf of Eilat coverage. Consequently, the two-site radial velocity measurements were objectively mapped directly using the Matlab OpenMA toolbox implementation of the procedure described by Kaplan and Lekien (2007). Because this method uses all available radial velocity information, possible spurious effects of spatial gaps on the mapping are minimized. A minimum spatial scale of 5 km was chosen, resulting in a set of 18 Dirichlet modes, 27 Neumann modes, and 21 boundary modes.

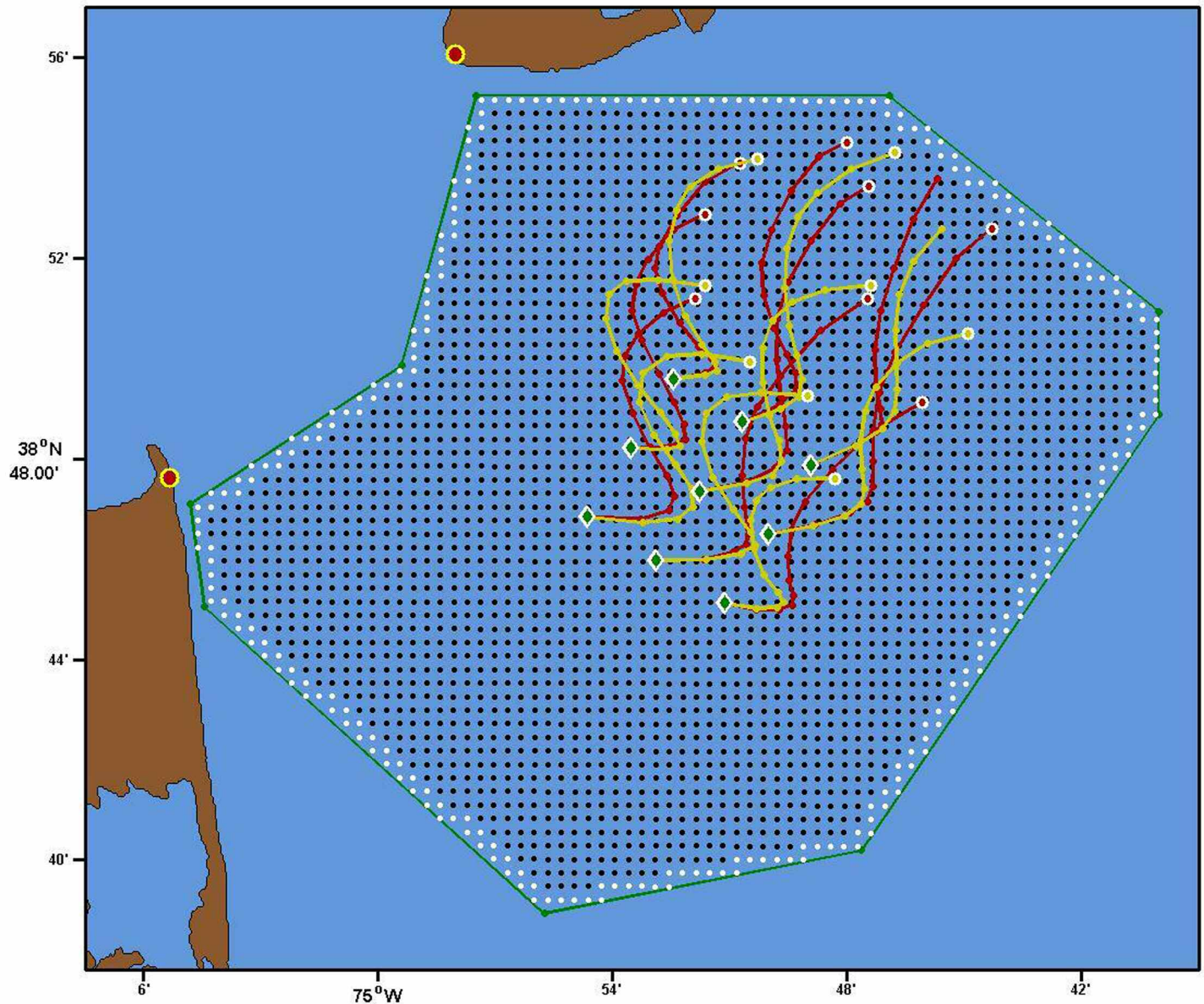


Fig. 2. Map of the Delaware Bay mouth showing the objective mapping domain (green), mapping grid points (black and white circles), and locations of the two radar sites (red circles). The nine particle launch positions for this study are shown as green diamonds with white outline. Example 12-hour trajectories (red) and PVD trajectories (yellow) for particles launched at 1200 UT on 12 April 2008 are also shown.

Computing trajectories and PVDs—For both analysis regions, trajectories and PVDs were computed from objective mappings of HF radar velocity measurements using Matlab code. The discrete ordinary differential path equations were integrated using an adaptive time-step Runge-Kutta scheme (Matlab's ode45 function). The coarsest time step was chosen to be the same as the HF radar archive time interval: 30 min for the Gulf of Eilat and 1 h for the Delaware Bay mouth. Velocities were interpolated when necessary using a bilinear scheme in space and a linear time interpolation scheme (Matlab interp function). Trajectory integrations required both space and time interpolation. In both regions, any trajectory/PVD pair was excluded from the

analysis if the trajectory reached the domain boundary or the PVD crossed over to land before they separated by 1 km. Because only horizontal velocity measurements were available, all computed paths are near surface and two dimensional, and vertical particle motion was ignored. No attempt was made to account for diffusive processes or to parameterize subgrid scale effects.

To compute PVDs, velocities over the entire integration time interval were chosen as the time-dependent velocities from the record at the PVD launch location. This is equivalent to assuming that the velocity field is spatially uniform, with time dependence specified by the velocity time series at the launch location.

Table 1. Gulf of Eilat monthly launch statistics and mean separation times (in hours).

	N_L	N_T	N_G	500 m			1000 m		
				Mean	95% interval		Mean	95% interval	
September 2005	162	82,620	49,177	5.32	5.30	5.34	7.08	7.06	7.11
October 2005	224	114,240	62,067	5.23	5.21	5.25	7.00	6.98	7.03
November 2005	216	110,160	51,144	5.30	5.27	5.32	7.02	6.99	7.04
December 2005	108	55,080	29,034	4.45	4.42	4.48	6.22	6.19	6.26
January 2006	76	38,760	18,971	6.06	6.02	6.10	7.51	7.46	7.56
February 2006	46	23,460	10,614	5.77	5.72	5.83	7.21	7.14	7.27
March 2006	205	104,550	48,283	6.28	6.26	6.31	7.94	7.91	7.96
April 2006	55	28,050	13,036	4.46	4.42	4.49	6.13	6.08	6.18
May 2006	164	83,640	48,307	5.23	5.21	5.26	6.99	6.96	7.02
June 2006	96	48,960	24,841	5.45	5.42	5.49	7.36	7.32	7.40
July 2006	192	97,920	59,032	5.45	5.43	5.47	7.28	7.25	7.30
August 2006	187	95,370	55,557	5.55	5.53	5.58	7.34	7.31	7.36
September 2006	107	54,570	31,464	5.46	5.44	5.49	7.21	7.18	7.25

N_L corresponds to the number of particle launches, N_T ($510 \times N_L$) corresponds to the total number of PVD/trajectory pairs computed, and N_G corresponds to the number of good PVD/trajectory pairs analyzed for each month.

In the Gulf of Eilat, because particle launch locations corresponded to OMA grid points, no spatial interpolation was necessary for PVD calculations. At the Delaware Bay mouth, where particle launch locations did not coincide with OMA grid points, PVD calculations required spatial interpolation, but *always to the particle launch location*.

In the Gulf of Eilat, particles were launched on a regular grid of 510 initial positions that correspond to the grid points of the OMA objective mapping (black dots in Fig. 1). Particles were launched every 3 h during each monthly analysis period and tracked for 12 h. Twelve example trajectories (red lines) and PVDs (yellow lines) are shown in Fig. 1. Temporal gaps in the radar coverage required careful choices for the span of each monthly analysis interval, to ensure that the archived velocity record was continuous when trajectories were computed. For each of the 13 months analyzed, the longest continuous velocity record interval for the month was chosen as the analysis period. Table 1 shows the number of particle launches (N_L), the total number of trajectories computed (N_T , equal to $510 \times N_L$), and the number of “good” PVD/trajectory pairs analyzed (N_G) for each month in the Gulf of Eilat. A trajectory/PVD pair was considered to be good if the pair remained within the boundary for the entire integration time, or if they separated by at least 1 km before the trajectory reached the domain boundary or the PVD crossed over to land. Table 1 shows that the 13 monthly analysis intervals ranged from 135 h (46 launches) in February 2006 to 669 h (224 launches) in October 2005.

At the Delaware Bay mouth, the analysis domain boundaries were mostly open, so particles could escape. To minimize particle escapes, we used a grid of nine initial positions near the center of the analysis domain (see Fig. 2). Particles were launched hourly over a 72-h analysis period in each month and tracked for up to 48 h. A total of 648 particles were

launched each month. A particle was considered to have escaped as soon as it entered any velocity grid cell that did not have valid velocities at all four cell corners. Temporal and spatial gaps in the radar coverage required careful choices for each monthly analysis interval. Because the radar coverage here had more spatial variability than the Gulf of Eilat, an additional criterion was used to ensure enough spatial coverage existed to constrain the OMA maps. For each hourly map in an analysis period, at least 65% of all mapping grid points were required to be *no further than 5 km* from a radial velocity measurement from *each radar site*. Most of the time, the spatial coverage was much better than this. Table 2 shows the time intervals (all times are UT) for each month of the 10-month analysis period (January through October 2008). For each monthly analysis period, Table 2 also shows the minimum value for the percentage of mapping grid points within 5 km of radial velocity measurements from each site (column labeled “Minimum %”).

Separation statistics—For all pairings of trajectories and PVDs, two simple statistics were computed: the time for the trajectory and PVD paths to separate by 500 m and 1000 m. Monthly mean separation times are reported for both analysis regions. Because the distributions of separation times had long tails (see Fig. 3), the 95% confidence interval for the monthly mean separation times was estimated using the nonparametric bootstrap method (Efron and Tibshirani 1986) with 1000 samples.

Assessment

The Gulf of Eilat—Fig. 3A and B shows histograms of the 500- and 1000-m separation times for all particles launched in September 2005. Note that the histograms show distributions with broad peaks and long tails. Because of these distribution shapes, the 95% confidence interval limits for the mean separation times were estimated using a bootstrap technique with

Table 2. Time intervals (all times are UT) for each month of the 10-month analysis period (January through October 2008).

	Start		End		Minimum % ^a
	Day	Hour	Day	Hour	
January	11	0200	16	0200	84.0
February	23	2300	28	2300	84.8
March	26	2300	31	2300	93.7
April	11	0300	16	0300	93.3
May	17	1000	22	1000	91.6
June	18	2300	23	2300	81.1
July	18	1200	23	1200	77.1
August	8	0000	13	0000	68.6
September	10	0000	15	0000	66.5
October	16	1000	21	1000	77.3

^aThe minimum value for the percentage of mapping grid points within 5 km of radial velocity measurements from each site.

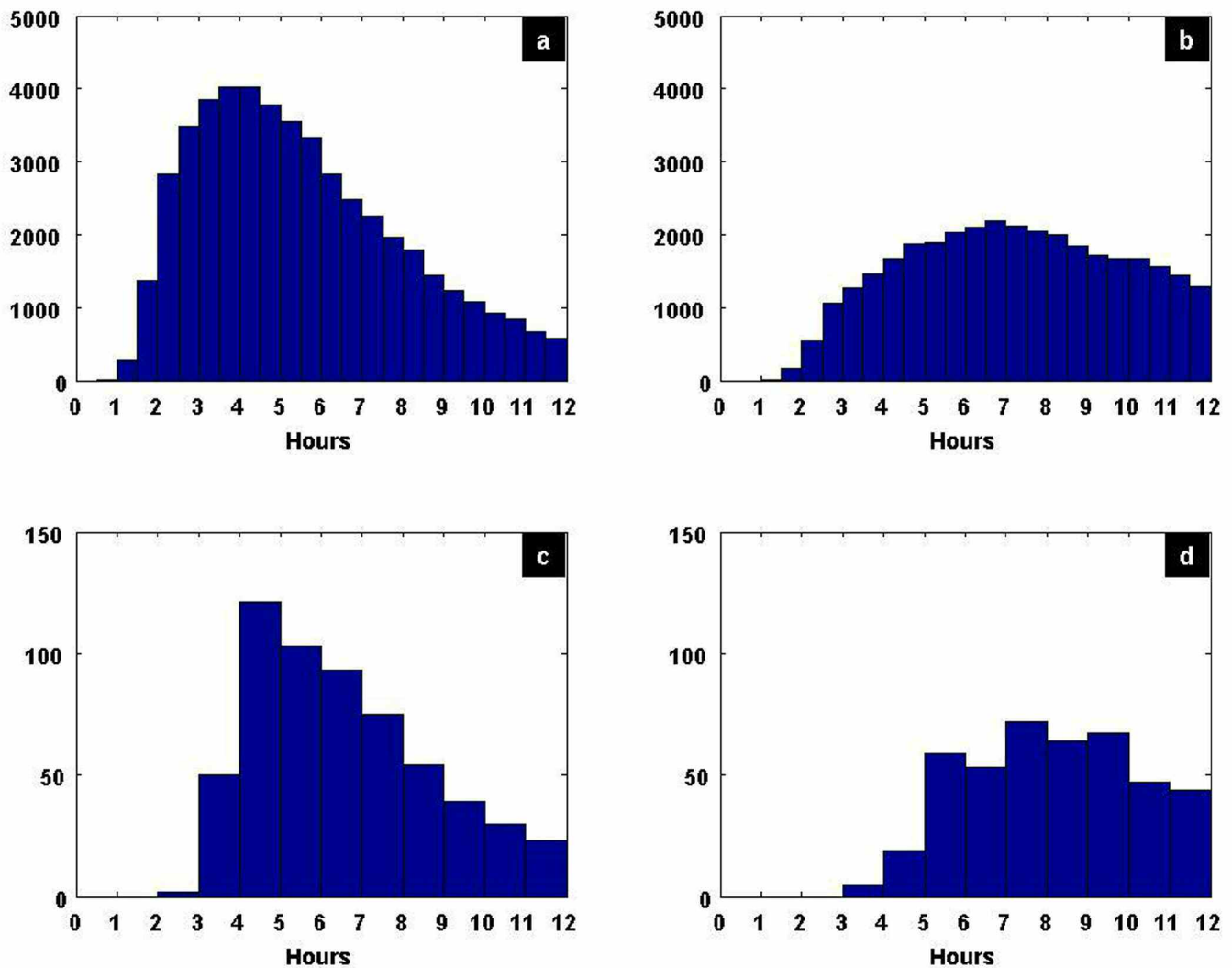


Fig. 3. Histograms of 500- and 1000-m separation times (hours) for September 2005 in the Gulf of Eilat (A and B) and for September 2008 at the Delaware Bay mouth (C and D). For both regions, other months studied here show similar distributions with broad peaks and long tails.

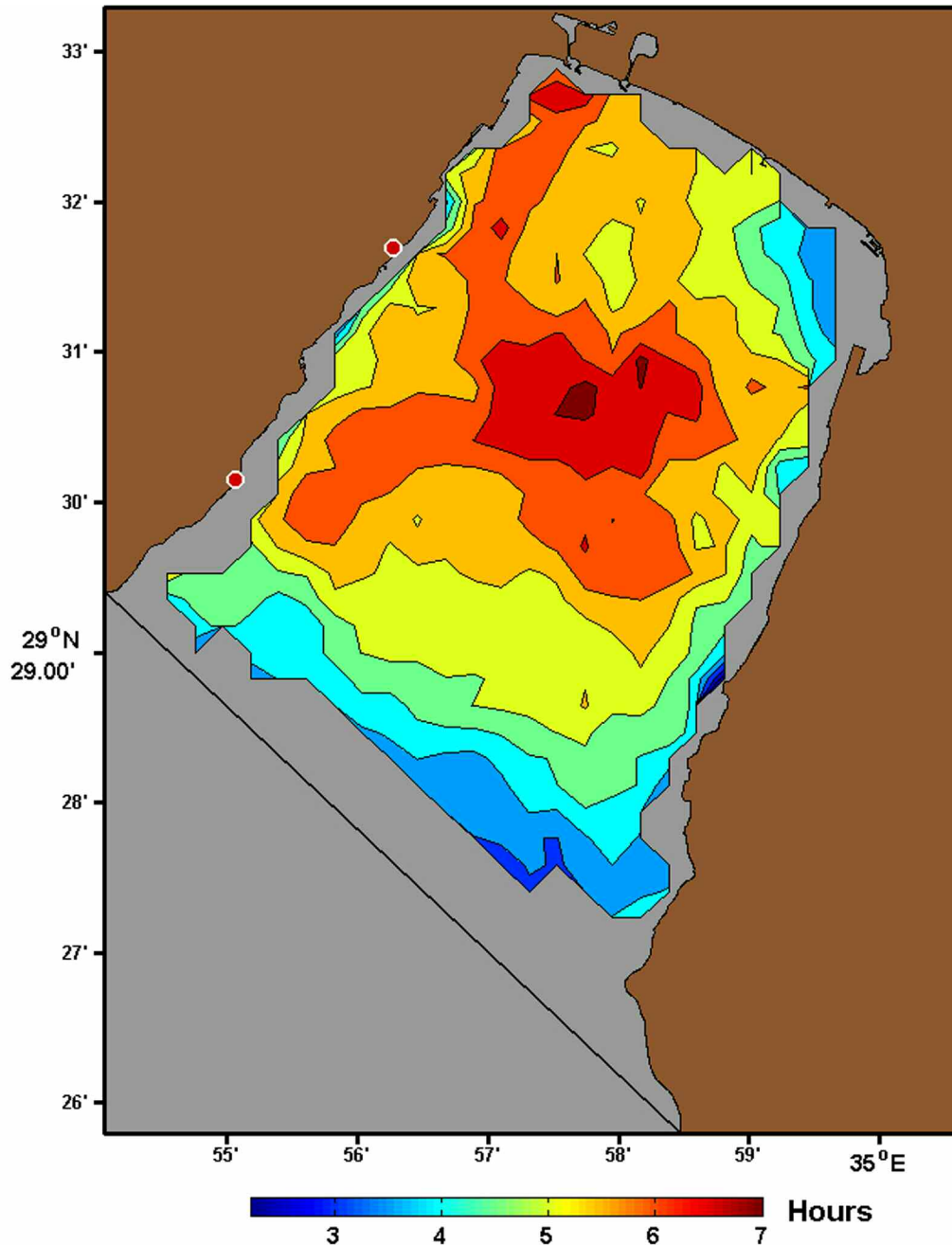


Fig. 4. Color contours of mean 500-m separation times (in hours) for the Gulf of Eilat in September 2005. The largest separation times occur in the center of the Gulf and in the northwest corner.

1000 samples. Table 1 shows monthly mean values of 500- and 1000-m separation times and 95% confidence interval limits for these mean values for the Gulf of Eilat. Table 1 indicates that the average time required for PVDs and trajectories to separate by 1000 m ranges from 6.13 to 7.94 h. The 500-m separation time ranges from 4.45 to 6.28 h.

Particle initial positions cover most of the Gulf of Eilat, allowing the spatial distribution of separation times to be examined. Figure 4 shows color contours of the mean 500-m

separation times for September 2005. Larger separation times occur near the center of the gulf and in the northwest corner. Larger values are expected in the center of the Gulf, since particles launched here are farthest from the coast. Near a land boundary, the flow typically changes direction over relatively short distances (as the flow veers alongshore), increasing the spatial gradients that drive the separation between trajectories and PVDs. An explanation for increased separation times in the northwest corner of the gulf is less clear, although it is

Table 3. Delaware Bay monthly mean separation times (in hours).

	500 m			1000 m		
	Mean	95% interval	Missing samples	Mean	95% interval	Missing samples
January 2008	4.93	4.75 5.11	0	7.81	7.51 8.11	0
February 2008	4.64	4.47 4.83	0	6.94	6.69 7.22	3
March 2008	5.19	5.04 5.34	0	7.45	7.22 7.68	0
April 2008	4.78	4.62 4.94	0	7.52	7.24 7.83	1
May 2008	4.79	4.63 4.96	0	7.59	7.31 7.88	2
June 2008	4.52	4.34 4.71	0	6.56	6.30 6.85	2
July 2008	4.09	3.97 4.21	0	6.18	5.97 6.40	4
August 2008	5.61	5.41 5.81	3	8.65	8.31 9.02	14
September 2008	6.90	6.66 7.14	0	10.20	9.88 10.54	2
October 2008	4.85	4.70 5.01	0	7.76	7.45 8.05	3

Particles that escaped the domain before 1000-m separation could occur were treated as missing samples.

likely that lower mean flow in this region reduces the separation rate between trajectories and PVDs, even when the coastline is nearby.

The Delaware Bay mouth—Table 3 shows monthly mean values of 500- and 1000-m separation times and 95% confidence interval limits for these mean values for the Delaware Bay mouth. The average 1000-m separation times range from 6.18 to 10.2 h and the average 500-m separation times range from 4.09 to 6.9 h. During some months, a small number of particles escaped the domain before they separated from the PVD by the specified distance. Escaped particles are considered as missing values, and the number of missing values is shown in Table 3. These should be compared with the total number of particle launches (648) in each month. Figure 3C and D shows histograms of the 500-m and 1000-m separation times for all particles launched in September 2008. Similar to the Gulf of Eilat results, these histograms show distributions with broad peaks and long tails. Again, the 95% confidence interval limits were estimated using the bootstrap technique.

Discussion

We assessed the accuracy of surface transport estimates based on PVDs using synoptic surface currents measured by HF radar in two coastal regions with distinctly different flow regimes over time intervals spanning several months. The errors that result from assuming that PVDs represent true particle trajectories (an assumption that is only strictly accurate when the currents are spatially uniform) were assessed by computing the times for PVDs and trajectories to separate by 500 and 1000 m. For both regions studied, PVDs deviate from true trajectories by 1000 m over time periods of less than 12 h (monthly mean values of 6–7.5 h for the Gulf of Eilat and 6–10.2 h for the Delaware Bay mouth). These monthly mean separation times do not vary significantly from month to month, suggesting that seasonal influences are minimal. It is noteworthy that these separation time statistics are so similar for two coastal regions with marked differences in surface circulation characteristics.

Because both trajectories and PVDs were computed using the same velocity archives and the same numerical algorithms, details about how they were computed cannot explain the separation of their paths. This separation is due solely to the spatial variability of the surface currents and the accumulating effect of this spatial variability as particles move over time.

Comments and Recommendations

Studies that involve surface transport in the coastal ocean focus on events spanning days to weeks, time periods over which significant net transport can occur. Because these results demonstrate that PVDs accumulate errors of 1 km or more during the first 12 h, they clearly cannot provide useful surface transport estimates over time periods longer than this. These results demonstrate that, although spatial variations in coastal surface currents may not be easily quantified by eye, their effect on trajectories is significant and develops rapidly over several hours. No simple remedy exists to salvage the PVD for applications involving coastal transport: where surface currents vary spatially, this variability must be measured or modeled, and its influence on particle paths must be explicitly accounted for when trajectories are computed.

References

- Barrick, D. E., B. J. Lipa, and R.D. Crissman. 1985. Mapping surface currents with CODAR. *Sea Technol.* Oct.:43-48.
- Ben-Tzvi, O., M. Kiflawi, H. Gildor, and A. Abelson. 2007. Possible effects of downwelling on the recruitment of coral reef fishes to the Eilat (Red Sea) coral reefs. *Limnol. Oceanogr.* 52:2618-2628.
- Berman, T., N. Paldor, and S. Brenner. 2000. Simulation of wind-driven circulation in the Gulf of Elat (Aqaba). *J. Mar. Sys.* 26:349-365.
- Berman, T., N. Paldor, and S. Brenner. 2003. Annual SST cycle in the eastern Mediterranean, Red Sea, and Gulf of Elat. *Geophys. Res. Lett.* 30(5), 1261. [doi:10.1029/2002GL015860].

- Efron, B., and R. Tibshirani. 1986. Bootstrap methods for standard errors, confidence intervals, and other measures of statistical accuracy. *Stat. Sci.* 1:54-77.
- Emery, W. J., and R. E. Thomson. 2001. *Data analysis methods in physical oceanography*, 2nd ed. Elsevier, 638 pp.
- Epifanio, C. E., A. K. Masse, and R. W. Garvine. 1989. Transport of blue crab larvae by surface currents off Delaware Bay, USA. *Mar. Ecol. Prog. Ser.* 54:35-41.
- Fiechter, J., B. K. Haus, N. Melo, C. N. K. Mooers. 2008. Physical processes impacting passive particle dispersal in the Upper Florida Keys. *Cont. Shelf Res.* 28:1261-1272.
- Genin, A., and N. Paldor. 1998. Changes in the circulation and current spectrum near the tip of the narrow, seasonally mixed Gulf of Eilat. *Isr. J. Earth Sci.* 47:87-92.
- Gildor, H., E. Fredj, J. Steinbuck, and S. Monismith. 2009. Evidence for submesoscale barriers to horizontal mixing in the ocean from current measurements and aerial-photographs. *J. Phys. Oceanogr.* 39:1975-1983.
- Gurgel, K.-W., H.-H. Essena, and S. P. Kingsley. 1999. High-frequency radars: Physical limitations and recent developments. *Coast. Eng.* 37:201-218.
- Kaplan, D. M., and F. Lekien. 2007. Spatial interpolation and filtering of surface current data based on open-boundary modal analysis. *J. Geophys. Res.* 112. [[doi:10.1029/2006JC003984](https://doi.org/10.1029/2006JC003984)].
- Kaplan, D. M., J. Largier, L. W. Botsford. 2005. HF radar observations of surface circulation off Bodega Bay (northern California, USA). *J. Geophys. Res.* 110. [[doi:10.1029/2005JC002959](https://doi.org/10.1029/2005JC002959)].
- Lekien, F., C. Coulliette, A. J. Mariano, E. H. Ryan, L. K. Shay, G. Haller, J. E. Marsden. 2005. Pollution release tied to invariant manifolds: A case study for the coast of Florida. *Physica D* 210:1-20.
- Lekien, F., and H. Gildor. 2009. Computation and approximation of the length scales of harmonic modes with application to the mapping of surface currents in the Gulf of Eilat. *J. Geophys. Res.* 114, C06024. [[doi:10.1029/2008JC004742](https://doi.org/10.1029/2008JC004742)].
- Lekien, F., C. Coulliette, R. Bank, and J. Marsden. 2004. Open-boundary modal analysis: Interpolation, extrapolation, and filtering. *J. Geophys. Res.* 109:C12004.
- Lipphardt, B. L. Jr, D. Small, A. D. Kirwan Jr, S. Wiggins, K. Ide, C. E. Grosch, and J. D. Paduan. 2006. Synoptic Lagrangian maps: Application to surface transport in Monterey Bay. *J. Mar. Res.* 64:221-247.
- Manasrah, R. S., F. A. Al-horani, M. Y. Rasheed, S. A. Al-roushan, and M. A. Khalaf. 2006. Patterns of summer vertical and horizontal currents in coastal waters of the northern Gulf of Aqaba, Red Sea. *Estuar. Coast Shelf Sci.* 69:567-579.
- Monismith, S. G., and A. Genin. 2004. Tides and sea level in the Gulf of Aqaba (Eilat). *J. Geophys. Res.* 109:C04015.
- Ogston, A. S., C. D. Storlazzi, M. E. Field, M. K. Presto. 2004. Sediment resuspension and transport patterns on a fringing reef flat, Molokai, Hawaii. *Coral Reefs* 23:559-569.
- Shadden, S. C., F. Lekien, J. D. Paduan, F. P. Chavez, J. E. Marsden. 2009. The correlation between surface drifters and coherent structures based on high-frequency radar data in Monterey Bay. *Deep Sea Res.* 56:161-172.
- Tomczak, M. 2000. Advanced exercises in physical oceanography. <http://www.es.flinders.edu.au/~mattom/IntExerc/advanced2/quest05.html> (Accessed Feb. 18, 2010).

Submitted 18 October 2009

Revised 19 December 2009

Accepted 13 January 2010